Research Square

Preprints are preliminary reports that have not undergone peer review.
They should not be considered conclusive, used to inform clinical practice,
or referenced by the media as validated information.

Clinical evidence of Kelch13-dependent and -independent malaria treatment failure with Artemether-Lumefantrine

Jacob Souopgui

Jacob.Souopgui@ulb.be

Universite Libre de Bruxelles - ULB https://orcid.org/0000-0003-1526-4431

Sandra Fankem

Université Libre de Bruxelles - ULB

Jean-Bosco Mbonimpa

King Faisal Hospital Rwanda

Edgar Kalimba

Université Libre de Bruxelles

Yvan Karuke

Uppsala University https://orcid.org/0000-0001-5210-9276

Mariama Diallo

Université Libre de Bruxelles

Article

Keywords:

Posted Date: July 25th, 2025

DOI: https://doi.org/10.21203/rs.3.rs-6958044/v1

License: This work is licensed under a Creative Commons Attribution 4.0 International License.
Read Full License

Additional Declarations: There is **NO** Competing Interest.

Clinical evidence of *Kelch13*-dependent and -independent malaria treatment failure with Artemether-Lumefantrine

Sandra Fankem Noukimi[1], Jean-Bosco Mbonimpa[2], Edgar Mutebwa Kalimba[1,2], Yvan Karuke[3], Mariama Telly Diallo[1], Jacob Souopgui[1,2]*

[1] Laboratory of Embryology and Biotechnology, Department of Molecular Biology, Faculty of Science, Université Libre de Bruxelles, Gosselies, Belgium; sandra.fankem.noukimi@ulb.be, edgar.kalimba@ulb.be, mariama.telly.diallo@ulb.be, Jacob.Souopgui@ulb.be

[2] Rwanda Malaria Research Lab, King Faisal Hospital Rwanda, Kigali, Rwanda; edgar.mk@kfhkigali.com, furerebosco@gmail.com,

[3] Uppsala University, Uppsala, Sweden; ykaruke@gmail.com

* Correspondence: Jacob.Souopgui@ulb.be ; Tel.: +32 2 650 9936

Abstract

Malaria remains a major public health threat, particularly in sub-Saharan Africa. In Rwanda, Artemether-Lumefantrine (AL; Coartem) has been the primary treatment for uncomplicated malaria, though its efficacy is increasingly in question. Using clinical data and *Plasmodium* biobanks from King Faisal Hospital Kigali, we analyzed 23 selected samples from patient with recurrent malaria. Genotyping confirmed recrudescence rather than reinfection. Following the initial AL treatment, 56.5% (microscopy) and 83.3% (qPCR) remained positive, with symptoms persisting. After a second treatment, positivity declined but was still notable. Sequencing analysis revealed widespread MDR1 Y184F mutations and cumulative *Pfkelch13* mutations, including H384R in the BTB/POZ domain, associated with treatment failure. Four failing strains lacked *kelch13* mutations, indicating alternative resistance mechanisms. These findings support the need for expanded genetic surveillance to preserve ACT efficacy.

Introduction

Malaria is a serious health concern for the inhabitants and health systems of countries in tropical regions where this disease is endemic. According to the World Health Organization (WHO), there were 263 million cases of malaria in 2023 globally, with 597,000 estimated deaths, with children under 5 years of age accounting for about 80% of all malaria related deaths [1]. In order to help reduce and manage disease burden, WHO recommends many control and treatment strategies including treatment of malaria patients with artemisinin-based combination therapies (ACTs), the current front-line treatment for *Plasmodium falciparum* malaria (the most virulent species responsible for the majority of deaths) [1]. ACTs are effective and well tolerated, and have been a cornerstone of progress in reducing the burden of malaria disease [2]. However, despite admirable progress in the first 15 years of this century, there has been difficulties in achieving malaria elimination, the most critical reasons being the resistance to insecticides and the emerging partial resistance to artemisinin and derivatives [3,4].

ACTs are made of a combination of a fast-acting artemisinin derivative with a longer-acting partner drug. The artemisinin derivative rapidly reduces the parasite burden by targeting the asexual blood stage of *Plasmodium falciparum* [5]. Meanwhile, the partner drugs, which include lumefantrine, amodiaquine, piperaquine, pyronaridine or mefloquine, provide sustained antimalarial activity to clear residual parasites and prevent recrudescence. Each partner drug has unique pharmacokinetic and pharmacodynamic properties, contributing to the combination's overall effectiveness. However, emerging resistance to both artemisinin and some partner drugs threatens the long-term efficacy of ACTs, necessitating continuous monitoring and alternative treatment strategies [5,6].

The mechanism by which *P. falciparum* parasites develop partial resistance to artemisinin has been associated to non-synonymous single nucleotide polymorphisms (SNPs) in *Kelch13* (*K13*) gene within the chromosome 13 [5,7]. Its structural feature comprises a 726-amino acids protein organized into three main domains - propeller/Kelch, BTB/POZ, and coiled coil-contained [8]. The first SNPs associated to malaria treatment failure were identified in the K13 propeller domain (K13PD) of clinical isolates in Southeast Asia [9,10]. These mutations have been spread throughout Sub-Saharan Africa, predominantly in countries in East Africa and the Horn of Africa, including Rwanda, Uganda and Eritrea [11–13]. The ability of *Plasmodium* parasite populations to evolve in response to interventions implies that ongoing surveillance is critical to monitor drug resistance. In the public health context, WHO validated 13 SNPs and proposed 9 SNPs candidates all in the K13PD considered as biomarkers of artemisinin resistance based on the *Plasmodium in vitro* or *in vivo* phenotypes coupled to the mutation frequency following 10 years (2010-2019) of ACTs treatment efficacy surveillance [1].

At the pharmacological level, the canonical mode of action of artemisinin is modelled in a way that K13 appears to control hemoglobin uptake in a cytostome-dependent manner by mediating the ubiquitination of partners that are components of the endocytic apparatus [14,15]. Hemoglobin degradation by the parasite digestive vacuole leads to the production of heme that catalyzes the activation of artemisinin and derived compounds into free radicals, resulting in protein damage, proteotoxicity and subsequently parasite death [15]. In this model, non-synonymous SNPs in the K13PD should modulate the

binding of the different substrates leading to less hemoglobin uptake, less heme production, less artemisinin and derivatives activation, and less protein damage, conferring partial resistance to these drugs.

Substrate ubiquitination is an evolutionarily conserved biochemical reaction mediated by the Cullin-3 (E3) Ligase complex that requires BTB/POZ and E3 ligase physical interaction [16,17]. Mutations in the BTB/POZ domain of K13 should therefore impair the binding interaction as well, leading to aberrant substrate ubiquitination. Hence, in the context of *Plasmodium* resistance to ACTs, mutations in this domain should also result in less hemoglobin degradation, thereby producing less activated artemisinin, leading to parasite partial resistance. Consistently, *in vitro* selection on a West African *P. falciparum* strain under a dose-escalating artemisinin regimen revealed enhanced parasite survival. This was associated with P413A SNP in the BTB/POZ domain. Using CRISPR/Cas9 editing techniques on a Dd2 parasite strain this mutation was found sufficient to induce artemisinin partial resistance *in vitro* [18]. Although not evidenced by clinical observations, this was an alert to scientists in this field, as well as health authorities to extend the screening of mutations associated to *P. falciparum* partial resistance beyond the propeller domain of K13.

Resistance to ACTs partner drugs arises through various molecular mechanisms that reduce the efficacy of these compounds, primarily by targeting the pathways critical to their mode of action. For example, lumefantrine (partner drug used in the unique first line treatment in Rwanda until 2024), amodiaquine and piperaquine, all face resistance driven by mutations in the *Plasmodium falciparum* chloroquine resistance transporter (*pfcrt*) and multidrug resistance 1 (*pfmdr1*) genes [5,19,20]. These mutations alter drug transport and accumulation within the parasite, thereby reducing drug efficacy [5]. Resistance to sulfadoxine-pyrimethamine (SP), mediated by point mutations in the dihydropteroate synthase (*dhps*) and dihydrofolate reductase (*dhfr*) genes, threatens the efficacy of intermittent preventive therapy in infant (SP-IPTi) and seasonal malaria chemoprevention (SMC) in young children [21–23]. There is thus a critical need for surveillance of resistance markers to help in the choice of effective malaria drugs.

In this study, we present data-driven evidence that the long-term, widespread use of Artemether-Lumefantrine (Coartem) for non-severe malaria in Rwanda has led to a significant decline in treatment efficacy, associated with the emergence of *Plasmodium falciparum* strains harbouring both Kelch13-dependent and Kelch13-independent single nucleotide polymorphisms (SNPs), including novel mutations such as H384R, which is linked to treatment failure.

Results

Efficacy of Artemether-Lumefantrine (Coartem) treatment on parasite load

Blood collected from hospital biobank was analyzed by microscopy and qPCR to detect the presence or absence of *Plasmodium* after treatment with Coartem. Out of the 23 patient samples, all were positive before treatment (BT) with microscopy and qPCR, with parasitemia ranging between 500 and 100.000 parasites/µL of blood as observed in figure1A. This was inversely proportional to CT values ranging from 11 to 35 as observed in figure1B. Additionally, we observed as shown in figure1 that 56.5% (microscopy) and 83.3% (qPCR) of samples remained positive after the first treatment and 28.6% and 51.7%

after second treatment (figure1B) with persistence of clinical symptoms of malaria. This suggests that Coartem failed to clear completely the parasite load 3 to 5 days after treatment. This treatment failure led to participants with residual parasites, resulting in what we called "ACT-induced" *Plasmodium falciparum* reservoirs that may help perpetuating the disease transmission.

To evaluate the transmissibility of the disease, we compared the expression level of *Plasmodium* gametocytes in blood samples collected before and after treatment, as gametocytes are the sexual stages responsible for transmission to mosquitoes. Total RNA was extracted from 16 blood samples with treatment failure and processed by RT-qPCR targeting the mature gametocyte specific marker *P25* gene (*Pfs25*), with the *Serine t-RNA syntethase* (*S-tRNA*) gene used as a *P. falciparum* housekeeping gene. The relative expression was calculated, and we observed a significant increase of *Pfs25* expression (P = 0.0014, Mann Whitney, 95% confidence interval), revealing a higher gametocyte number upon treatment, which corroborate with microscopic observations in figure 1C.

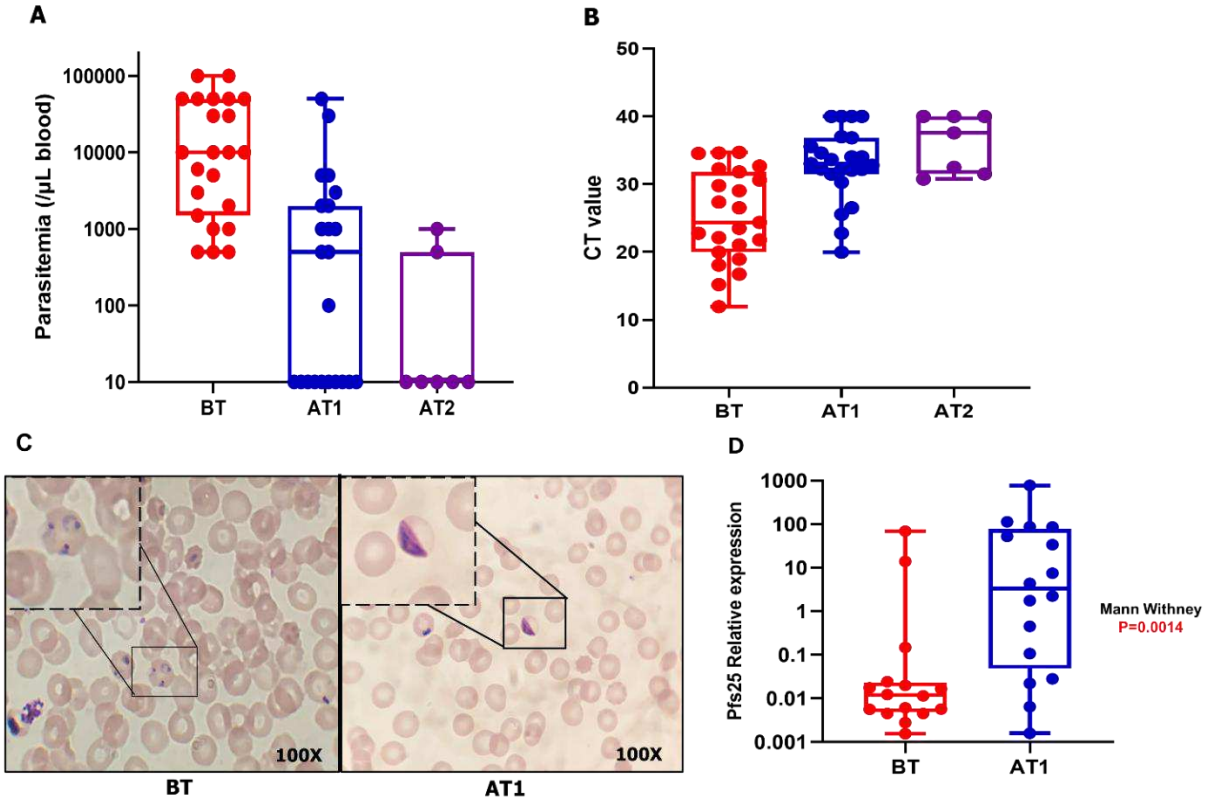

Figure 1: Efficacy of Artemether-Lumefantrine (Coartem) on *P. falciparum* clinical isolates. Parasite load was evaluated before and after treatments with Coartem through microscopy (**A**), and qPCR (**B**). Total gDNA was extracted and the qPCR performed targeting the *Pf* 18SrRNA gene. Malaria thin blood smear from a participant before and after treatment with Coartem (**C**), mainly ring stage *P. falciparum* (*P.f*) before treatment and gametocytes after treatment as shown in a high magnification picture (see black boxes). Relative expression of *PfS25* in 16 participants before and after treatment by RT-qPCR. The *Serine t-RNA synthe*tase (*S-tRNA*) was used as a *P. falciparum* housekeeping gene (**D**). The relative expression was calculated and compared before and after treatment using Mann Whitney test at 95% confidence interval (P = 0.0014) upon treatment. BT – before treatment, AT1- after first treatment and AT2- after second treatment represent time point of sample collection.

To confirm if parasites detected after treatment failure were residual parasites from last infection (recrudescence) and not a new infection (reinfection), *Merozoite Surface Protein 2* (*MSP2*), a highly polymorphic gene, was genotyped using Sanger sequencing method. During this, agarose gel revealed the presence of co-infection in some clinical isolates

marked by the presence of double bands, suggesting two strains with different sizes of *MSP2* genes, which was subsequently confirmed by Sanger sequencing (figure S1). Finally, Pairwise analysis of mono-infected *MSP2* sequence before and after treatment (figure S2) revealed conserved sequence identity in isolates before and after Coartem treatments, supporting the process of recrudescence rather than reinfection.

Next, drug resistance markers were evaluated by amplifying as illustrated in Figure S3A and sequencing key genetic markers associated with antimalarial resistance, namely *crt, mdr1, dhfr, dhps* and *kelch13* genes whose coverage depth using Oxford Nanopore Technology (ONT) platform is shown in Figure S3B. VCF files obtained after processing ONT data were analysed and revealed the presence of at least one resistance marker of 4-aminoquinoline in 86.9% as shown in figure 2A, specifically 13.04% (3 out of 23) having K76T mutation on *crt* gene and 86.9% (20 out of 23) having Y184F mutation on *mdr1*, both being WHO-validated markers of drug resistance.

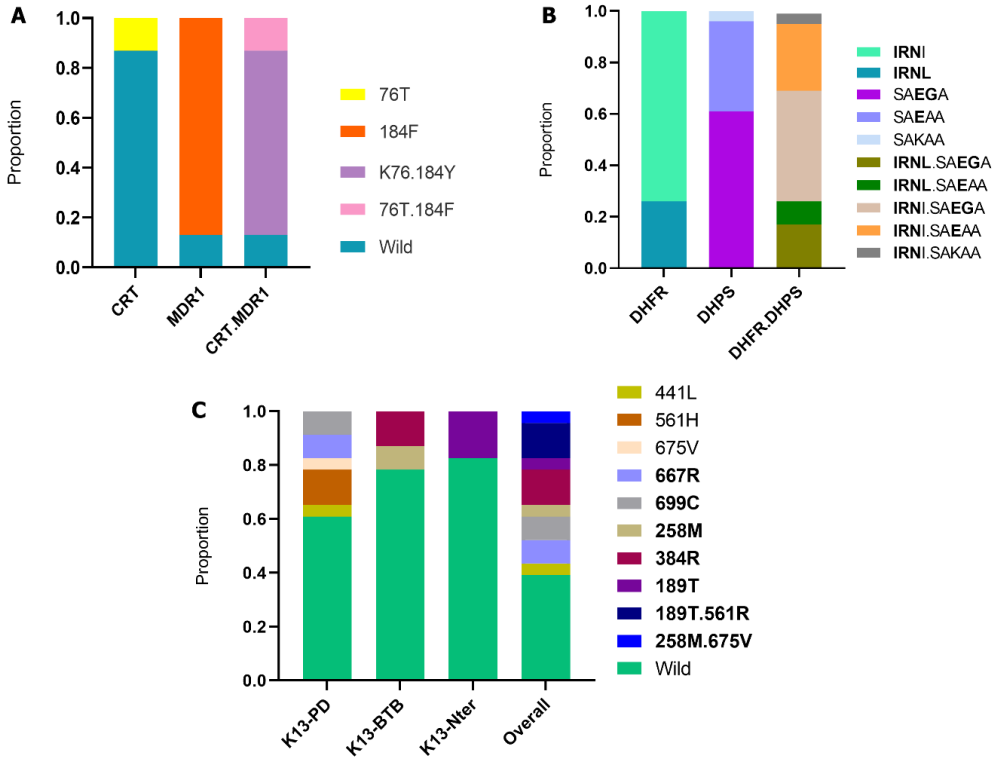

Figure 2 : Frequency distribution of single nucleotide polymorphism (SNP) in (A) CRT and MDR1, (B) DHFR and DHPS and (C) KELCH 13 domains. DHFR haplotypes correspond to amino acid positions 51, 59, 108 and 164 (wild type, NCSI) and DHPS haplotypes correspond to amino acid positions 436, 437, 540, 581 and 613 (wild type, SAKAA).

Regarding antifolates drug resistance markers (figure 2B), haplotype combination in *dhfr* were the triple mutant **IRN**I (73.9%, 17 out of 23)and the quadruple mutant **IRNL** (26.1%, 6 out of 23) which refers to amino acid positions 51, 59, 108 and 164 (with 108N, the main allele to pyrimethamine resistance). The 3 haplotypes identified in *dhps* were SA**EG**A (60.8%, 14 out of 23), SA**E**AA (34.8%, 8 out of 23), and the wild type SAKAA (4.3%, 1 out of 23) which *refers* to amino acid positions 436, 437, 540, 581 and 613. The *dhfr* and *dhps* haplotype combinations were *dhfr*-**IRN**I + *dhps*-SA**EG**A (43.5%), *dhfr*-**IRN**I + *dhps*-SA**E**AA (26.1%), *dhfr*-**IRNL** + *dhps*-SA**EG**A (17.4%, N=23) and other haplotypes (13%, N=23). A haplotype combination specifically associated with decreased efficacy of both sulfadoxine and pyrimethamine *dhfr*-**IRNL** + *dhps*-K540E was observed in 26.1% (N=23).

Artemisinin molecular markers of resistance were assessed by sequencing all the 3 domains of the gene as described in figure 2C. In the propeller domain where all WHO-validated mutations have been reported, we identified two WHO-validated markers, namely R561H mutation (3 out of 23, 13.05%), and A675V (1 out of 23, 4.34%), one WHO-candidate marker, P441L (1 out of 23, 4.34%), and two emerging SNPs namely P667R (2 out of 23, 8.7%) and F699C (2 out of 23, 8.7%). The BTB/POZ domain revealed the presence of 2 SNP – L258M (2 out of 23, 8.7%) and H384R (3 out of 23, 13.05%) – while the N-terminal showed K189T SNP (4 out of 23, 17.4%). Unexpectedly, cumulative mutations were revealed in couple of cases. All mutations identified in kelch13 were validated by sanger sequencing as shown in figure S4.

Early treatment failure correlation with artemisinin drug resistance markers

In depth investigation of molecular markers of resistance based on treatment success or early treatment failure is presented in Table 1. We found that Coartem treatment success correlated with the absence of mutations in the *Kelch 13* gene in four cases. Secondly, our investigations revaled the presence of P441L, P667R and F699V in 5.3%, 10.5% and 10.5%, respectively in samples from patients with failure after first treatment.

Table 1: Antimalarial drug resistance markers frequency with respect to treatment outcome.

Gene	SNP	T1-success, n(%) total N=4	T1-failure, n(%) total N=19	T2-failure, n(%) total N=4
crt	K76T	0	3 (15.8%)	0
	Wild	4 (100%)	16 (84.2%)	4 (100%)
mdr1	Y184F	4 (100%)	16 (84.2%)	3 (75%)
	Wild	0	3 (15.8%)	1 (25%)
dhfr	N51I	4 (100%)	19 (100%)	4 (100%)
	C59R	4 (100%)	19 (100%)	4 (100%)
	I108N	4 (100%)	19 (100%)	4 (100%)
	I164L	1 (25%)	5 (26.3%)	2 (50%)
	Wild	0	0	0
dhps	K540E	3 (75%)	19 (100%)	4 (100%)
	A581G	2 (50%)	12 (63.2%)	2 (50%)
	Wild	1(25%)	0	0
Kelch13	K189T	0	0	0
	L258M	0	0	1 (25%)
	H384R	**0**	**3 (15.8%)**	**2 (50%)**
	P441L	0	1 (5.3%)	0
	P667R	0	2 (10.5%)	0
	F699C	0	2 (10.5%)	0
	K189T.R561H	**0**	**3 (15.8%)**	**0**
	L258M.A675V	0	1 (5.3%)	0
	Wild	**4 (100%)**	**5 (26.3%)**	**1 (25%)**

The table describes frequency of alternative allele and the frequency of the allele in brackets. T1-success represents the group of patients who was negative with qPCR after treatment, T1-failure the group who was positive after the first treatment and T2-failure the group who was positive after second treatment

Notably, the validated R561H marker was present in group of patients with treatment failure after first treatment but was always coupled with mutation in the N-terminal K189T.

This suggests that an association of both SNPs could be required for more pronounce resistance. Moreover, the H384R mutation present in the BTB/POZ domain was observed both in group with first treatment failure (15.8%, N=19) and second treatment failure (50%, N=4). These findings strongly support the hypothesis of potential markers of resistance in the BTB/POZ domain. Finally, the absence of any mutation in *kelch 13* gene from group with failure after first (26.3%) and second (25%) treatment suggests the existence of *Kelch13*-independent malaria treatment failure with Artemether-Lumefantrine (Coartem).

To correlate efficacy decrease of Coartem with the presence of molecular markers of resistance, combination of mutations in *kelch13* (associated with artemisinin partial resistance), *crt* and *mdr1* (associated to partner drug resistance such as lumefantrine) was determined across each individual sample (figure 3). We could clearly correlate the success of Coartem treatment in T1-success clinical isolates (sample P7, P16, P17 and P22) with absence of mutation in *kelch13* gene despite the presence of Y184F mutation associated to lumefantrine resistance. Unexpectedly, some isolates in T1-failure (sample P9, P2, P1, P6 and P8) and T2-failure (sample P2) with no mutation in *kelch13* gene instead showed a resistant profile. This suggests the presence of other genes and mechanisms associated with artemisinin partial resistance.

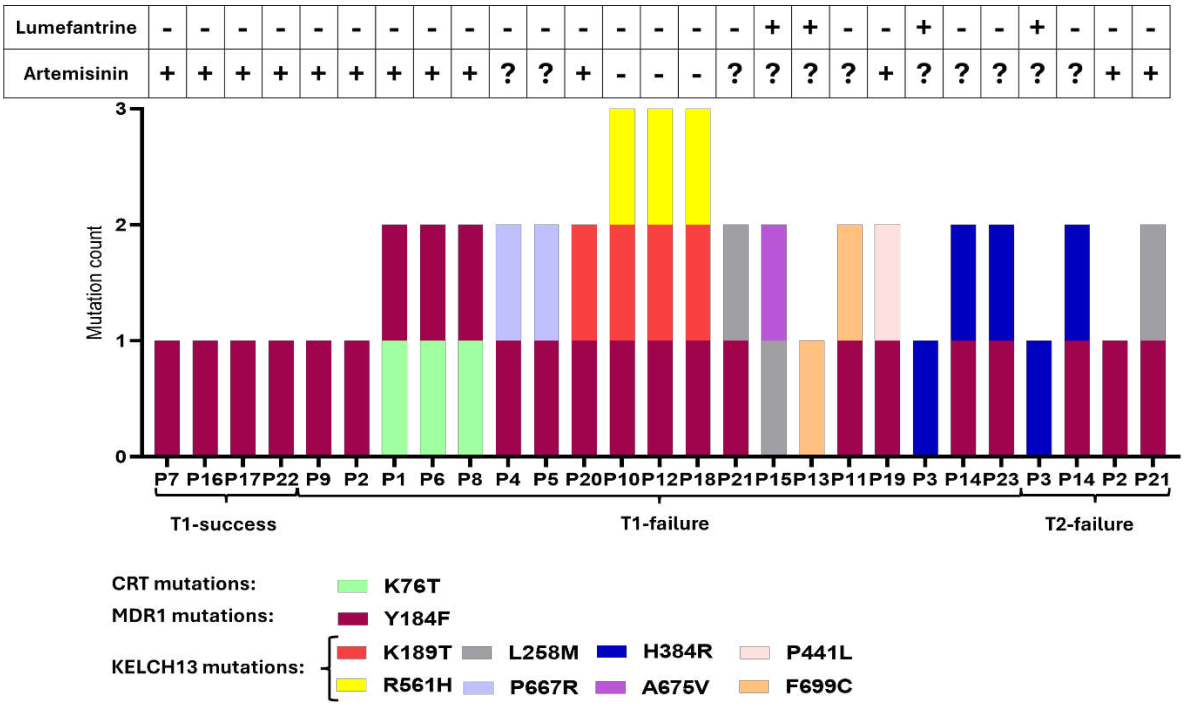

Figure 3: Distribution of mutations across all 23 samples in *crt, mdr1* and *Kelch13* genes. Combination of mutations in *kelch13, crt* and *mdr1* was correlated with treatment success and failure. Phenotypes of lumefantrine and artemisinin were also observed with (+) being sensitive phenotype, (-) resistant phenotype and (?) unknown phenotype. T1-success represents the group of patients whose sample was negative by qPCR after treatment, T1-failure the group of those whose sample was positive after the first treatment and T2-failure the group who remained positive after second treatment.

All mutations (single and double mutations) observed in all 3 domains of *kelch13* gene were associated with clinical treatment failure. Principally, H384R mutation present in BTB/POZ domain was observed both in T1-failure (sample P3, P14 and P23) and T2-failure (sample P3 and P14) groups. Remarkably, in addition to the combined R561H and K189T mutations observed in samples P10, P12, and P18, cumulative SNPs were also detected in the *kelch13* gene of sample P15. This finding warrants close surveillance, as such

strains may exhibit enhanced fitness and an increased potential for drug resistance. Finally, Y184F mutation associated to lumefantrine resistance was observed in 20 out of 23 (86.9%) samples. This reveals that the malaria first line treatment in Rwanda, namely Coartem (artemether + lumefantrine) principally may depend on the artemisinin moiety only as lumefantrine molecular marker of resistance is detected in 86.9% (N = 23) of isolates.

In silico prediction of protein interaction between H384R Kelch13 protein and Cullin E3-ubiquitin ligase complex

The Kelch13 BTB/POZ and Propeller domain (figure 4A) and the Cullin-E3 ligase complex (figure 4B) crystallographic structure were retrieved from the Protein Data Bank (PDB) repository. After introduction and validation of H384R mutation illustrated using the AlphaFold 3 Server as shown in figure 4A, molecular docking was performed using the Haddock 2.4 webserver. Interaction between wild type H384 Kelch 13 protein and Cullin E3 ligase complex revealed a root mean square deviation (RMSD) of 1.1. This indicates a high similarity between the two residues, as well as reduces distance between atoms in the binding pocket (figure 4C). On the contrary, interaction between H384R-mutant and Cullin ligase revealed an increase RMSD to 23.1. This drastic increase in RMSD suggests that the introduction of mutation increased distance between atoms in the binding pocket (figure 4D) and thus decreasing the stability of the interaction. Additionally, increase in binding energy (table S1) of complex from H384R Kelch 13 and cullin-E3 may reflect a decrease in stability as compared to the wildtype protein.

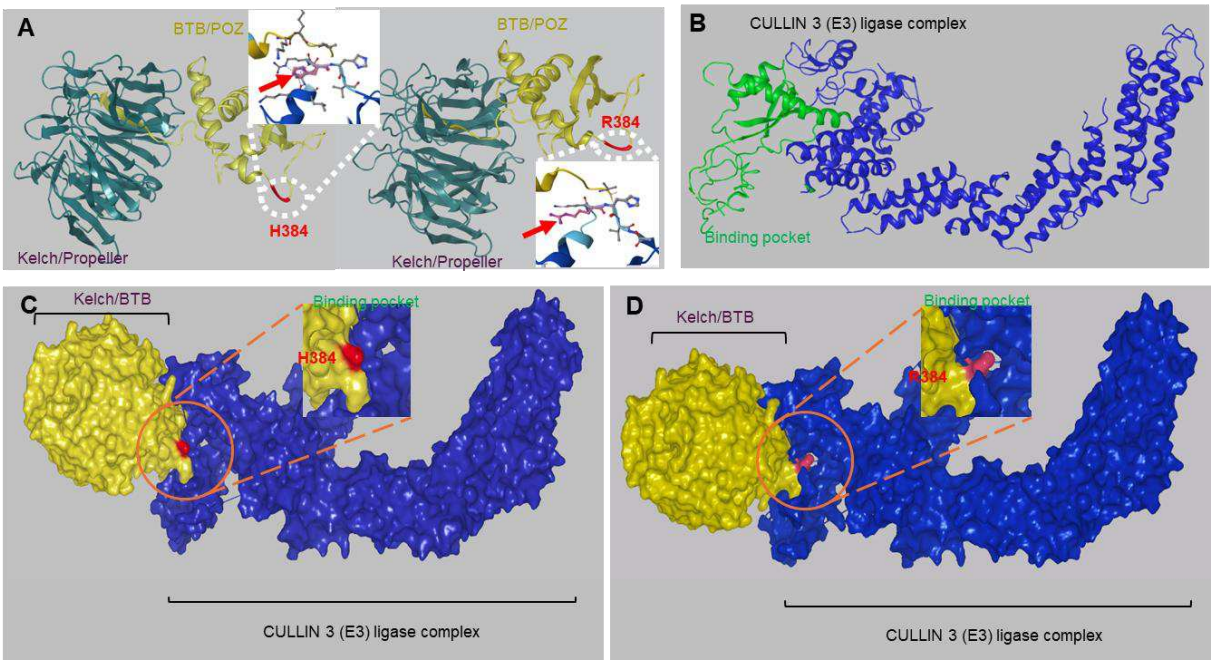

Figure 4: Molecular docking of H384R single nucleotide polymorphism (SNP) in the BTB/POZ and CULLIN 3 (E3) ligase complex. (**A)** Wild type and mutant *PfKelch13* BTB/POZ domain in yellow and Propeller domain in dark green with the respective H384 and 384R residues highlighted in red and detailed using AlphaFold 3 Server. (**B)** Location of the binding pocket in green within the Cullin-2 and E3 ubiquitin ligase monomers. The rest of Cullin-2 E3 ligase complex structure is shown in blue. **(C)** Docked complex of Cullin-2 E3 Ubiquitin ligase with H384 wild type Kelch 13 and **(D)** 384R mutant Kelch 13.

Discussion

Our results provide clinical evidence of Artemether-Lumefantrine (Coartem) treatment failure at King Faisal Hospital in Kigali. Following anecdotal reported recurrent malaria cases by the physicians of the hospital, we analysed data and samples from the hospital biobank from patients who exhibit symptoms despite series of treatment with Coartem. From a set of 23 samples selected for this study, a high prevalence of clinical treatment failure reaching 56.5% and 83.3% by microscopy and qPCR, respectively, was obtained (figure 1). These findings are consistent with reports of emerging artemisinin resistance in African countries such as Rwanda, Tanzania, and Uganda [12,24]. Although clinical evidence of treatment failure to ACT has not been widely confirmed in Africa [25], our study outcomes unveiled for the first time the presence of *Plasmodium falciparum* strains with genetic architecture supporting resistance to Coartem in Rwanda.

Despite the limited sample size of 23 clinical isolates, it should be foreseen that these reported ACT-induced *P. falciparum* strains will fuel disease persistence as such resistant alleles will spread throughout the communities. Consistently, to assess the potential transmissibility of *P. falciparum* variants we analysed the expression of the gametocyte-specific gene *PfS25* before and after treatment. Our results (figure 1D) showed an increase in *PfS25* expression post-treatment, suggesting elevated gametocyte levels following Coartem treatment. This correlates with findings from Vietnam, Burkina Faso and Mozambique [26], where increased sexual conversion rates were reported in *Plasmodium* parasites following artemisinin-based treatment. Moreover, a study conducted in Indonesia demonstrated that participants treated with dihydroartemisinin-piperaquine combined with a single dose of primaquine, a known anti-gametocyte drug, had significantly lower gametocyte loads as compared to cohort receiving the only dihydroartemisinin-piperaquine [27]. This supports our findings and reinforces the notion that ACT may promote gametocyte differentiation, potentially enhancing the transmission potential of drug-resistant parasites in the absence of a gametocytocidal agent. These results underscore the importance of integrating transmission-blocking strategies, such as the addition of primaquine, particularly in regions where ACT efficacy is declining and resistance is emerging.

We genotyped drug resistance markers and our results (figure 2A) indicates trends towards an increase of chloroquine susceptibility of 85.8% compared to 50% in 2015 [28]. This most probably reflects shifts in national treatment policy, as chloroquine was phased out due to resistance and artemether-lumefantrine became the first-line antimalarial treatment in Rwanda. Increasing chloroquine susceptibility has also been observed in Africa [29,30]. However, a high prevalence of Y184F (20 out of 23, 86.9%) (figure 2A) which is associated to lumefantrine resistance has been observed like in Uganda, the neighbouring country [30]. This mutation is reported to increase lumefantrine tolerance in the combination therapy [31,32]. As a result of this, artemether-lumefantrine (Coartem) treatment efficiency may depend solely on the artemisinin moiety. Hence, the Rwanda government opted to add dihydroartemisinin-piperaquine and artesunate-pyronaridine in the national malaria treatment guidelines as the second-line for treatment of uncomplicated malaria cases [33]. Given the lower prevalence of mutations in *crt* gene (3 out of 23, 13%) in this study, and also from the fact that artemether, artesunate and dihydroxyartemisinin, all have the same mode of action linked to the endoperoxide bridge [5], it could be advantageous in the current situation in Rwanda to switch completely from

artemether-lumefantrine to these two new ACTs as they are anticipated to be more effective thanks to their partner drugs.

The dhfr-IRNI triple mutant (73.9%) parasites is consistent with previous results from Rwanda [28] ,northern Ghana and Uganda [30]. We also observed a high prevalence of SA**EG**A (60.8%), SA**E**AA (34.8%) parasites. In Rwanda, SP (sulfadoxine-pyrimethamine) is included into the malaria treatment policy as a prophylaxis in pregnancy and under 5-year-old children, thus, ongoing exposure of parasites to SP may be driving the persistence and/or rise of resistant alleles in *dhfr* and *dhps*.

A total of 8 SNPs were identified on all 3 domains of *Kelch 13* gene with 2 WHO-validated markers – R561H (13.05%) and A675V (4.34%), and 1 WHO-candidate marker - P441L (4.34%). This aligns with other studies in Rwanda, where the R561H mutation was found at 7.5% in 2015 [11] and 9% in 2019 [34]. However, in our results, R561H SNP was systematically linked with K189T mutation (samples P10, P12 and P18), generating the first haplotype observed in *Kelch 13 gene,* all experienced treatment failure with Coartem (figure 3). However, in an unpublished cross-sectional work from our team, R561H appears independently of K189T, although most of the samples harboured both mutations simultaneously. The presence of these two mutations could result from drug pressure driving adaptive mutations in the parasite or from the crossing of two strains carrying these mutations during the mosquito's sexual development. Moreover, two other emerging SNPs were detected in the study participants among which P667R and F699C both at 8.7% that have not yet been reported in Rwanda and is associated with treatment failure (samples P4, P5, P11 and P13).

Our study also revealed the presence of parasite that did not have any mutation in the *Kelch 13* gene. After investigating individual genotype per sample (figure 3), kelch13 sensitive genotype was observed in T1-success group (sample P7, P16, P17 and P22) – the group that had no residual parasite after one treatment. However, malaria symptoms were observed by medical doctor after treatment, supporting the need to assess other pathologies characterized by symptoms like those of malaria. Consistently, in tropical settings, malaria share common symptoms with other infectious diseases [35,36] and this could explain the presence of the symptoms. Moreover, we identified five samples from T1-failure (sample P1, P2, P6, P8 and P9) and one samples from the T2-failure (sample P2) groups with sensitive kelch13 genotype but failed to successfully clear parasite after treatment with Coartem like the T1-success group. This contradictory finding strongly suggests that another mechanism could be directly linked with clinical artemisinin. Such K13-independent drug resistance suggests the presence of mutations in other genes of the canonical pathway [37] currently modelled to explain the artemisinin resistance. These genes might be the regulator of haemoglobin uptake by endocytosis and this is in line with other studies which demonstrated that *Plasmodium in vitro* delay parasite clearance was associated with genes other that *Kelch 13,* involved in the endocytosis pathway [14,15,37,38] with evidence of potential clinical delay clearance observed in rodents [39,40] to support the hypothesis.

Finally, the H384R single nucleotide polymorphism (SNP) located in the BTB/POZ domain of PfK13 was detected in 13.04% of the analysed samples of this study (samples P3, P14 and P23). This finding aligns with previous *in vitro* studies that have reported delayed parasite clearance associated with SNP within this domain [18]. However, to date, no SNP

in the BTB/ POZ domain of *PfK13* has been conclusively linked to clinical treatment failure. Our study presents the first evidence suggesting a potential association between the H384R mutation and clinical ACT treatment failure. This observation raises important questions regarding the functional role of the BTB/POZ domain. This domain has been hypothesized to mediate direct interaction with the Cullin E3 ubiquitin ligase complex, a key component in protein degradation and stress response pathway [8], mutation such as H384R could plausibly alter the function of the PfK13 protein and contribute to reduced drug susceptibility. Further molecular and functional characterization of the H384R variant is therefore warranted to clarify its role in resistance mechanisms and to assess its potential as a molecular maker of ACT treatment failure.

Molecular docking simulations comparing the interaction between the H384 and Culin-E3 ligase complex and the 384R and Culin-E3 ligase revealed the increase of RMSD from 1.1 with wild protein to 23.1 in mutant. Substitution of histidine (imidazole group) to an arginine (guanidinium group) reflected a decrease in atoms present in the binding pocket, thus decreasing the stability of the interaction. However, these are preliminary analysis and thus, further *in silico* and *in vitro* analysis should be performed to validate H384R as a marker of ACT resistance.

In summary, while recent reviews have downplayed clinical ACT resistance globally, our findings revealed clear evidence of clinical treatment failure of Artemether-Lumefantrine (coartem) in Rwanda, highlighting the importance of monitoring treatment efficacy in real-world settings. Moreover, our findings suggest that ACT resistance may not be solely associated to mutations in the propeller domain of *Kelch 13* gene. Notably, we report an association between the H384R mutation in BTB/POZ domain of the Kelch13 protein and clinical treatment failure, highlighting a potentially overlooked region in the molecular surveillance of artemisinin resistance. Importantly, our data also indicate that ACT treatment may promote gametocyte differentiation, thereby increasing the potential of transmission of parasite strains carrying both known and potentially novel resistance-associated mutations. These results underscore the urgent need for comprehensive genomic surveillance to monitor the evolution and spread of resistant *Plasmodium falciparum* in Rwanda and beyond borders.

Methods

Description of the study

Between October 2021 and June 2023, we carried out a malaria study at King Faisal Hospital (reference hospital in Rwanda) in response to concerns raised by medical doctors about recurrent malaria cases. To investigate this, we examined a set of 23 samples from the hospital biobank, identified as cases of suspected malaria recrudescence. These samples were initially collected by the hospital laboratory based on medical doctors requests, with all testing positive for malaria by microscopy and/or RDT. The patients were prescribed Coartem, but after 3 to 5 days, all the 23 cases continued to exhibit persistent malaria symptoms. This prompted a second round of malaria diagnostics using microscopy and rapid diagnostic tests (RDT), to confirm or not positivity. Positive patients were treated again with Coartem, yet some continued to present malaria symptoms. A third diagnosis confirmed the persistence of malaria, leading to a second treatment with Coartem in those cases. Blood collected from hospital

biobank before (BT), after first (AT1) and second (AT2) treatments was transported in DNA/RNA Shield (Zymo Research) in Belgium for further molecular analysis.

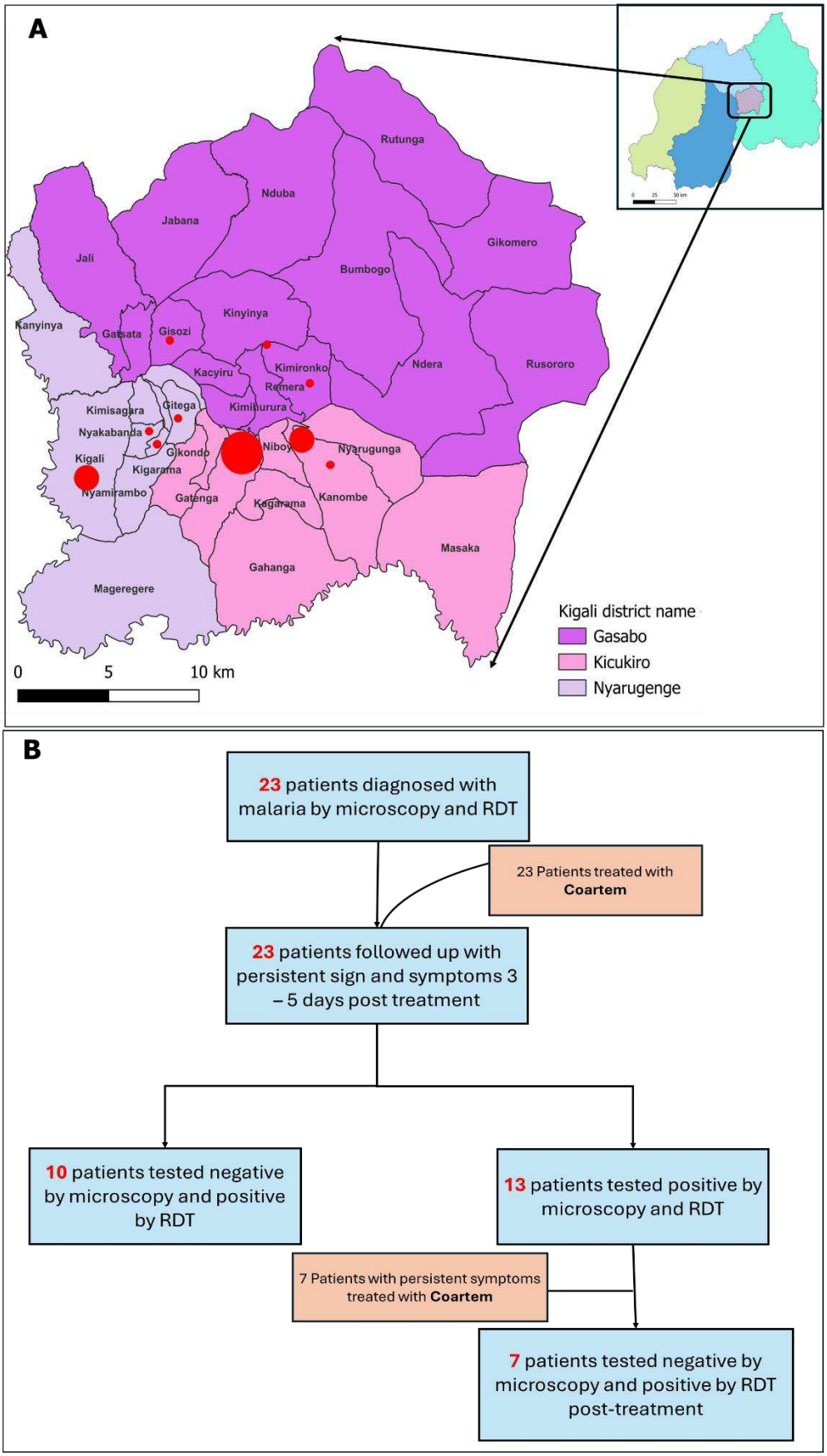

Figure 5: Residence location (A) and flow diagram (B) of patients involved in the study. A total of 23 malaria positive patients with recurrent episodes were selected out of 267 patients enrolled at the King Faisal Hospital in Kigali between October 2021 and June 2023, coming from various city of the capital (red circles representing the proportion of participant living in an area, mapped with QGIS 3.42.3).

Venous blood collected for diagnosis purposes were used for molecular analysis. Sample was collected prior to treatment with Coartem as prescribed by their medical doctor. About 3 to 5 days after treatment due to persistence of symptoms, participant's blood was collected and 13 out of 23 tested positive by microscopy and RDT. After first dose of treatment, 7 out of 13 patients still had persistent malaria symptoms and upon doctor request blood was collected for diagnosis and were prescribed with a second dose of Coartem.

Nucleic acid extraction and molecular analysis

Total genomic DNA and RNA were extracted from blood collected during the study using Maxwell® RSC Whole Blood DNA Kit (Promega – AS1520) and Maxwell® RSC SimplyRNA Blood Kit (Promega – AS1380) respectively. qPCR targeting 18s ribosomal RNA gene was performed on the LightCycler 480® machine (Roche) to quantify of parasite present in the blood samples. *MSP2* gene characterising *P. falciparum* strains was amplified by PCR and products were revealed on 2% agarose gels, purified and sequenced using Eurofins genomics platform. Total RNA extracted was processed by RT-qPCR using the mature gametocyte specific marker P25 gene (*Pfs25*). The Serine t-RNA synthase (*S-tRNA*) gene was used as a *P. falciparum* housekeeping gene and relative expression of *Pfs25* calculated. Primers pairs used are presented in supplementary table S2.

Genotyping of *P. falciparum* drug resistance markers, multiplex PCR of *crt, mdr1, dhfr, dhps* and *Kelch13* genes was performed as described previously with slight modification [41]. PCR products were revealed on a 2% agarose gel (figure S4) and library preparation performed using Ligation sequencing amplicons - Native Barcoding Kit 24 V14 (SQK-NBD114.24) from Oxford Nanopore Technology (ONT, UK). Prepared library was run on Flongle Flow Cells (R10.4.1) for 24hrs using MinKNOW software version 24.06.16 (ONT, UK). Raw fastq files generated were trimmed to remove adapters using Porechop version 0.2.4 (https://github.com/rrwick/Porechop). NanoFilt tool version 2.8.0 [42] was used to filter reads with quality score < 10. The trimmed and filtered reads were mapped on *P. falciparum* 3D7 reference genome using Minimap2 software version 2.28-r1209 [43], generating a SAM file. BAM statistics, filtration, sorting, and indexing was done using different Samtools version 1.21 [44] functionalities (flagstat, view, sort, and index) to obtain sorted Bam and their indexes. BAM quality control was performed using the Qualimap software version 2.2.2 [45] and BAM files were visualized using IGV software version 2.16.0 [46]. Variance calling was performed using Clair3 Clair3 version *1.0.10* [47] haploid calling by including --include_all_ctgs , --haploid_sensitive and –gvcf parameters**.** The SNPs in gVCFs were filtered by quality (>10) and depth (>20) using bcftools version 1.21 [44] and annotation to extract SNPs information was performed using snpEff version 4.10 [48]. All data generated were analysed and plotted using GraphPad Prism version 8.

All *kelch13* sequences observed by ONT sequencing were confirmed using Sanger sequencing. This technique was also used to analyse the *merozoite surface protein* 2 (*msp2*) polymorphic marker to discriminate recrudescence and reinfection in the study samples. Briefly, *kelch 13* and *msp2* PCR were performed as described above using primer pairs in table S1. PCR product was purified using Wizard® SV Gel and PCR Clean-Up System (Promega – A9281) according to manufacturer's instruction. Purified product was then diluted and mixed with forward primer and sent for sequencing to Eurofins genomics. Fasta sequences generated were aligned using DNA Star software.

***In silico* prediction of effect of H384R mutation**

The *PfKelch13* BTB/POZ and Propeller domain crystallographic structure was retrieved from the Protein Data Bank (PDB) repository (PDB ID: **4yy8** and **5n4w** respectively). *In silico* modelling of the H384R mutation was performed using a combination of, AlphaFold 3 Server, DNA Star version 17 and Pymol Mutagenesis software (https://pymol.org/2/) and validation of the new structure was done subsequently. A Ramachandran plot was obtained from the PROCHECK server [49], a program that analyses residue and final structure geometry to check the stereochemical quality of a protein structure. The specific residues involved in the interactions were predicted using the CPORT server for the wild type, mutant protein. Validation of both the mutant and wild type structures was performed initially using the ProSA-Web server which calculates the input structure model's score and relates it to a range of scores that are typical for native proteins of similar sizes [50]. Subsequent validation was performed using the ERRAT server, which analyses patterns of non-bonded atom interactions relative to reliable crystallographic structures. The VERIFY server was used to assess the three-dimensional folding of the structure relative to its amino acid sequence [51], and molecular docking was then performed using the Haddock 2.4 web-server [52].

Ethics statement

The study was conducted in accordance with the Declaration of Helsinki and approved by the Rwandan National Ethics Committee (120/RNEC/2022). Informed consent was obtained from all patients or their parents or guardians involved in the study. In addition, written informed consent has been obtained from the malaria patient(s) at university hospital King Faisal Hospital Rwanda to publish this paper.

Data availability

The datasets generated during and/or analysed during the current study are available from the corresponding author on reasonable request. The sequence data has been submitted to the NCBI database and is currently under review. The accession number will be provided and included in the publication once the review process is complete

References

1. WHO. World malaria report. Geneva: World Health Organisation, 2024.

2. Bhatt S, Weiss DJ, Cameron E *et al*. The effect of malaria control on Plasmodium falciparum in Africa between 2000 and 2015. *Nature* 2015;**526**:207–11.

3. Suh PF, Elanga-Ndille E, Tchouakui M *et al*. Impact of insecticide resistance on malaria vector competence: a literature review. *Malar J* 2023;**22**:19.

4. Stokes BH, Dhingra SK, Rubiano K *et al*. Plasmodium falciparum K13 mutations in Africa and Asia impact artemisinin resistance and parasite fitness. Soldati-Favre D (ed.). *eLife* 2021;**10**:e66277.

5. Wicht KJ, Mok S, Fidock DA. Molecular Mechanisms of Drug Resistance in Plasmodium falciparum Malaria. *Annu Rev Microbiol* 2020;**74**:431–54.

6. Klein EY. Antimalarial drug resistance: a review of the biology and strategies to delay emergence and spread. *Int J Antimicrob Agents* 2013;**41**:311–7.

7. Ariey F, Witkowski B, Amaratunga C *et al*. A molecular marker of artemisinin-resistant Plasmodium falciparum malaria. *Nature* 2014;**505**:50–5.

8. Coppée R, Jeffares DC, Miteva MA *et al*. Comparative structural and evolutionary analyses predict functional sites in the artemisinin resistance malaria protein K13. *Sci Rep* 2019;**9**:10675.

9. Noedl H, Se Y, Schaecher K *et al*. Evidence of Artemisinin-Resistant Malaria in Western Cambodia. *N Engl J Med* 2008;**359**:2619–20.

10. Dondorp AM, Nosten F, Yi P *et al*. Artemisinin Resistance in Plasmodium falciparum Malaria. *N Engl J Med* 2009;**361**:455–67.

11. Uwimana A, Legrand E, Stokes BH *et al*. Emergence and clonal expansion of in vitro artemisinin-resistant Plasmodium falciparum kelch13 R561H mutant parasites in Rwanda. *Nat Med* 2020;**26**:1602–8.

12. Balikagala B, Fukuda N, Ikeda M *et al*. Evidence of Artemisinin-Resistant Malaria in Africa. *N Engl J Med* 2021;**385**:1163–71.

13. Schmedes SE, Patel D, Dhal S *et al*. Plasmodium falciparum kelch 13 Mutations, 9 Countries in Africa, 2014–2018. *Emerg Infect Dis* 2021;**27**:1902–8.

14. Birnbaum J, Scharf S, Schmidt S *et al*. A Kelch13-defined endocytosis pathway mediates artemisinin resistance in malaria parasites. *Science* 2020;**367**:51–9.

15. Xie SC, Ralph SA, Tilley L. K13, the Cytostome, and Artemisinin Resistance. *Trends Parasitol* 2020;**36**:533–44.

16. Wang P, Song J, Ye D. CRL3s: The BTB-CUL3-RING E3 Ubiquitin Ligases. *Adv Exp Med Biol* 2020;**1217**:211–23.

17. Furukawa M, He YJ, Borchers C *et al*. Targeting of protein ubiquitination by BTB–Cullin 3–Roc1 ubiquitin ligases. *Nat Cell Biol* 2003;**5**:1001–7.

18. Paloque L, Coppée R, Stokes BH *et al*. Mutation in the Plasmodium falciparum BTB/POZ Domain of K13 Protein Confers Artemisinin Resistance. *Antimicrob Agents Chemother* 2022;**66**:e0132021.

19. Valderramos SG, Fidock DA. Transporters involved in resistance to antimalarial drugs. *Trends Pharmacol Sci* 2006;**27**:594–601.

20. Mairet-Khedim M, Leang R, Marmai C *et al*. Clinical and In Vitro Resistance of Plasmodium falciparum to Artesunate-Amodiaquine in Cambodia. *Clin Infect Dis* 2021;**73**:406–13.

21. Cairns M, Ceesay SJ, Sagara I *et al*. Effectiveness of seasonal malaria chemoprevention (SMC) treatments when SMC is implemented at scale: Case-control studies in 5 countries. *PLoS Med* 2021;**18**:e1003727.

22. Baba E, Hamade P, Kivumbi H *et al*. Effectiveness of seasonal malaria chemoprevention at scale in west and central Africa: an observational study. *The Lancet* 2020;**396**:1829–40.

23. WHO. Global Malaria Programme: Intermittent preventive treatment for infants using sulfadoxine-pyrimethamine (IPTi-SP) for malaria control in Africa. Geneva, 2011.

24. Straimer J, Gandhi P, Renner KC *et al*. High Prevalence of Plasmodium falciparum K13 Mutations in Rwanda Is Associated With Slow Parasite Clearance After Treatment With Artemether-Lumefantrine. *J Infect Dis* 2022;**225**:1411–4.

25. Rosenthal PJ, Asua V, Bailey JA *et al*. The emergence of artemisinin partial resistance in Africa: how do we respond? *Lancet Infect Dis* 2024;**24**:e591–600.

26. Portugaliza HP, Natama HM, Guetens P *et al*. Plasmodium falciparum sexual conversion rates can be affected by artemisinin-based treatment in naturally infected malaria patients. *eBioMedicine* 2022;**83**:104198.

27. Sutanto I, Suprijanto S, Kosasih A *et al*. The effect of primaquine on gametocyte development and clearance in the treatment of uncomplicated falciparum malaria with dihydroartemisinin-piperaquine in South sumatra, Western indonesia: an open-label, randomized, controlled trial. *Clin Infect Dis Off Publ Infect Dis Soc Am* 2013;**56**:685–93.

28. Kateera F, Nsobya SL, Tukwasibwe S *et al*. Molecular surveillance of *Plasmodium falciparum* drug resistance markers reveals partial recovery of chloroquine susceptibility but sustained sulfadoxine-pyrimethamine resistance at two sites of different malaria transmission intensities in Rwanda. *Acta Trop* 2016;**164**:329–36.

29. Lu F, Zhang M, Culleton RL *et al*. Return of chloroquine sensitivity to Africa? Surveillance of African Plasmodium falciparum chloroquine resistance through malaria imported to China. *Parasit Vectors* 2017;**10**:355.

30. Tumwebaze PK, Conrad MD, Okitwi M *et al*. Decreased susceptibility of Plasmodium falciparum to both dihydroartemisinin and lumefantrine in northern Uganda. *Nat Commun* 2022;**13**:6353.

31. Konaté-Touré A, Gnagne AP, Bedia-Tanoh AV *et al*. Increase of Plasmodium falciparum parasites carrying lumefantrine-tolerance molecular markers and lack of South East Asian pfk13 artemisinin-resistance mutations in samples collected from 2013 to 2016 in Côte d'Ivoire. *J Parasit Dis* 2024;**48**:59–66.

32. Lobo E, de Sousa B, Rosa S *et al*. Prevalence of pfmdr1 alleles associated with artemether-lumefantrine tolerance/resistance in Maputo before and after the implementation of artemisinin-based combination therapy. *Malar J* 2014;**13**:300.

33. Mbabazi J. Rwanda rolls out new malaria strategy after recording 87,000 cases in March. *New Times* 2025.

34. van Loon W, Schallenberg E, Igiraneza C *et al*. Escalating Plasmodium falciparum K13 marker prevalence indicative of artemisinin resistance in southern Rwanda. *Antimicrob Agents Chemother* 2023;**68**:e01299-23.

35. Mahdavi SA, Raeesi A, Faraji L *et al*. Malaria or flu? A case report of misdiagnosis. *Asian Pac J Trop Biomed* 2014;**4**:S56–8.

36. Clark IA, Alleva LM, Mills AC *et al*. Pathogenesis of Malaria and Clinically Similar Conditions. *Clin Microbiol Rev* 2004;**17**:509–39.

37. Behrens HM, Schmidt S, Spielmann T. The newly discovered role of endocytosis in artemisinin resistance. *Med Res Rev* 2021;**41**:2998–3022.

38. Henrici RC, van Schalkwyk DA, Sutherland CJ. Modification of pfap2µ and pfubp1 Markedly Reduces Ring-Stage Susceptibility of Plasmodium falciparum to Artemisinin In Vitro. *Antimicrob Agents Chemother* 2019;**64**:e01542-19.

39. Simwela NV, Hughes KR, Roberts AB *et al*. Experimentally Engineered Mutations in a Ubiquitin Hydrolase, UBP-1, Modulate In Vivo Susceptibility to Artemisinin and Chloroquine in Plasmodium berghei. *Antimicrob Agents Chemother* 2020;**64**:e02484-19.

40. Henriques G, Martinelli A, Rodrigues L *et al*. Artemisinin resistance in rodent malaria - mutation in the AP2 adaptor µ-chain suggests involvement of endocytosis and membrane protein trafficking. *Malar J* 2013;**12**:118.

41. Girgis ST, Adika E, Nenyewodey FE *et al*. Drug resistance and vaccine target surveillance of Plasmodium falciparum using nanopore sequencing in Ghana. *Nat Microbiol* 2023;**8**:2365–77.

42. De Coster W, D'Hert S, Schultz DT *et al*. NanoPack: visualizing and processing long-read sequencing data. *Bioinformatics* 2018;**34**:2666–9.

43. Li H. New strategies to improve minimap2 alignment accuracy. *Bioinformatics* 2021;**37**:4572–4.

44. Danecek P, Bonfield JK, Liddle J *et al*. Twelve years of SAMtools and BCFtools. *GigaScience* 2021;**10**:giab008.

45. Okonechnikov K, Conesa A, García-Alcalde F. Qualimap 2: advanced multi-sample quality control for high-throughput sequencing data. *Bioinformatics* 2016;**32**:292–4.

46. Robinson JT, Thorvaldsdóttir H, Winckler W *et al*. Integrative genomics viewer. *Nat Biotechnol* 2011;**29**:24–6.

47. Zheng Z, Li S, Su J *et al*. Symphonizing pileup and full-alignment for deep learning-based long-read variant calling. *Nat Comput Sci* 2022;**2**:797–803.

48. Cingolani P, Platts ,Adrian, Wang ,Le Lily *et al*. A program for annotating and predicting the effects of single nucleotide polymorphisms, SnpEff: SNPs in the genome of Drosophila melanogaster strain w1118; iso-2; iso-3. *Fly (Austin)* 2012;**6**:80–92.

49. Laskowski R, Macarthur MW, Moss DS *et al*. PROCHECK: A program to check the stereochemical quality of protein structures. *J Appl Crystallogr* 1993;**26**:283–91.

50. Wiederstein M, Sippl MJ. ProSA-web: interactive web service for the recognition of errors in three-dimensional structures of proteins. *Nucleic Acids Res* 2007;**35**:W407–10.

51. Bowie JU, Lüthy R, Eisenberg D. A method to identify protein sequences that fold into a known three-dimensional structure. *Science* 1991;**253**:164–70.

52. Honorato RV, Koukos PI, Jiménez-García B *et al*. Structural Biology in the Clouds: The WeNMR-EOSC Ecosystem. *Front Mol Biosci* 2021;**8**:729513.

Acknowledgements

This research was funded by the Belgian university cooperation agency, Académie de Recherche et de l'Enseignement Supérieur (ARES), grant number Grant PFS2020-Rwanda to J.S.; the Rwanda Malaria Research Lab at King Faisal Hospital Rwanda (KFHR) in Kigali is cofounded by KFHR Foundation and the Elsa Miller Foundation to E.M.K.; The Ph.D. candidates S.F.N. and M.T.D. were fellows of the organization, Amis des Instituts Pasteur de Bruxelles (AIPB-asbl).

Author contributions

J.S. and S.F.N. contributed to the conceptualisation of the study and obtention of the ethical approval. E.M.K.; S.F.N. and J.B.M. performed sample collection and participant follow up. All experiments and data analysis were performed by S.F.N.; J.B.M.; Y.K. and M.T.D. under the supervision of J.S. Manuscript was prepared by S.F.N., edited and revised by J.S. for publication.

Competing interests

All authors declare there is no competing interests as defined by Nature Portfolio.

Supplementary Files

This is a list of supplementary files associated with this preprint. Click to download.

- supplementaryfigureFankemNS.pdf